Multistream Heat Exchanger Modeling and Design

Harry A. J. Watson, Kamil A. Khan, and Paul I. Barton
Massachusetts Institute of Technology, Process Systems Engineering Laboratory, Cambridge, MA 02139

DOI 10.1002/aic.14965
Published online August 4, 2015 in Wiley Online Library (wileyonlinelibrary.com)

A new model formulation and solution strategy for the design and simulation of processes involving multistream heat exchangers (MHEXs) is presented. The approach combines an extension of pinch analysis with an explicit dependence on the heat exchange area in a nonsmooth equation system to create a model which solves for up to three unknown variables in an MHEX. Recent advances in automatic generation of derivative-like information for nonsmooth equations make the method tractable, and the use of nonsmooth equation solving methods make the method very precise. Several illustrative examples and a case study featuring an offshore liquefied natural gas production concept are presented which highlight the flexibility and strengths of the formulation. © 2015 American Institute of Chemical Engineers *AIChE J*, 61: 3390–3403, 2015
Keywords: heat transfer, design (process simulation), mathematical modeling, simulation, process

Introduction

Despite being ubiquitous in cryogenic processes, multistream heat exchangers (MHEXs) are notoriously difficult to model, simulate, and design. Such processes are by nature extremely energy intensive, and therefore stand to benefit greatly from accurate process optimization. However, without effective and flexible models for heat exchange unit operations, accurate simulation and optimization of these processes cannot be performed. Among those cryogenic processes which utilize MHEXs, liquefied natural gas (LNG) production plants are of key importance in the current global energy industry. Due in part to the discoveries of large supplies of recoverable shale gas in North America, interest in natural gas as a primary fuel source has increased substantially in recent years. However, as natural gas must be compressed or liquefied for transport in an economically viable manner over distances greater than around 2000 miles (or around 700 miles for the case of offshore gas),[1] the final market price is a strong function of the cost of the liquefaction operation. Indeed, on average, this processing contributes around 52% of the total supply cost of natural gas (adding around $1-2 per MMBTU to the final market cost).[2] Base-load LNG plants typically employ multistream spiral-wound heat exchangers, the internal mechanisms of which are generally proprietary, and the performance of which are usually determined empirically. This application alone presents a compelling case for the development of general, rigorous, and versatile models for MHEXs for process design and simulation.

The use of process simulation software is common in the literature involving processes with MHEXs. Commercial simulators employ proprietary models which generally permit solving for a single unknown variable, afforded by the energy balance, typically taken as the one of the exchanger outlet temperatures. However, as an example, the first author's experience using the MHEATX block from Aspen Plus ®[3] suggests there are no rigorous checks in place to avoid heat exchange between two streams at very similar temperatures, or prevent temperature crossovers. This leads to the somewhat frustrating experience of needing to know parameter values which avoid this problem a priori, which then leads to a "guess-and-check" iterative approach to the MHEX simulation.

A more rigorous approach to modeling MHEX involves the use of a superstructure concept.[4,5] This approach works by deriving a network of two-stream heat exchangers which is equivalent to the MHEX. This model can also handle phase changes along the length of the heat exchanger, as long as the phase changes are known to happen a priori. The major disadvantage of this methodology is that simulating the MHEX involves the solution of a nonconvex mixed-integer nonlinear program model, which is extremely challenging to find globally, and would be highly undesirable to use within an outer optimization routine when the simulation is needed as part of a repeated function evaluation.

Another method for MHEX modeling borrows heavily from pinch analysis and the analysis of composite curves. A recent paper by Kamath et al.[6] showed how to create a fully equation-oriented model for MHEX by considering the unit operation as a heat exchanger network that requires no external utilities. The authors use the classic Duran and Grossmann[7] formulation for heat integration in their model, which will be more thoroughly discussed in the following section. They also show how their model can detect and handle phase changes through a disjunctive representation of the phase detection problem, and also that their model is amenable to cubic equations of state governing the thermodynamics. We note that the simulation and/or design of MHEX here again cannot be performed independently of solving a hard optimization problem.

Correspondence concerning this article should be addressed to P. I. Barton at pib@mit.edu.

Figure 1. Schematic of a countercurrent two-stream heat exchanger.

[Color figure can be viewed in the online issue, which is available at wileyonlinelibrary.com.]

A common theme in both the Kamath et al. article and much of the literature on pinch analysis is the use of smoothing approximations to remove the nondifferentiability inherent in the model, often with the formulation presented by Balakrishna and Biegler.[8] Alternatively, some authors choose to use the disjunctive mixed-integer model of the pinch operator from Grossmann et al.[9] Both these approaches introduce small, sensitive, user-set, non-physical parameters which can easily create numerical difficulties and inaccuracies. However, with the recent advent of robust methods for solving nonsmooth equation systems and optimizing nonsmooth functions,[10–13] such approximations are no longer a necessary evil, and the current work develops a model which handles nondifferentiable functions directly. This relies heavily on the use of tractable, automatic methods for calculating derivative-like information, more information about which is found in the following section.

It is also notable that the MHEX modeling literature rarely makes mention of the dependence of heat exchange area on the performance of the operation. Rather, it is often assumed that an exchanger of sufficient size is simply available, and the size is only calculated following determination of the output stream states, if at all. With the above discussion in mind, this article develops a new model and solution procedure for MHEX which solves for up to three unknowns, avoids returning infeasible solutions, does not rely on approximations or solving a hard optimization problem, and incorporates information about the available heat exchange area into the procedure. This model and the proposed solution method can be used both in a standalone unit operation model for use in a sequential-modular process simulation, or as the solution algorithm and part of the equation system in an equation-oriented simulation. An example of the latter functionality is shown in a case study for an offshore LNG production process later in the article. As a design tool, this model is intended for use at the flowsheeting stage of design for processes involving one or more MHEX units in order to determine stream states and evaluate feasibility. The detailed equipment design necessary before constructing MHEXs is not considered in this article (nor is it in any of the previously cited literature).

Background

Standard models for heat exchangers

We begin the development of the new model for MHEX by analogy to the well-known model of a countercurrent two-stream heat exchanger as shown in Figure 1. Here, a hot stream with (assumed) constant heat capacity flow rate F is cooled from inlet temperature T^{in} to outlet temperature T^{out} by exchanging heat with a cold stream with (assumed) constant heat capacity flow rate f, which in turn is heated from inlet temperature t^{in} to outlet temperature t^{out}.

The standard formulation of the model describing the transfer of heat in the exchanger shown in Figure 1 is given by the following equations:

$$F(T^{in}-T^{out})=f(t^{out}-t^{in}), \tag{1}$$

$$Q \equiv F(T^{in}-T^{out})=UA\Delta T_{LM}, \tag{2}$$

where Eq. 1 is the energy balance and Eq. 2 gives the relationship between the total heat transferred Q and the overall heat transfer coefficient U, the heat transfer area A and the log-mean temperature difference ΔT_{LM} (average driving force of heat transfer). Additionally, there exists a third relationship which governs this system but is generally not explicitly considered:

$$\Delta T_{min}=\min\{T^{in}-t^{out}, T^{out}-t^{in}\}, \tag{3}$$

where we will refer to ΔT_{min} as the minimum temperature difference or the minimum approach temperature. Explicitly defining ΔT_{min} in this manner is nonstandard. In practice, this quantity is often considered a parameter set a priori, which is then used after Eqs. 1 and 2 are solved to judge the feasibility of the result. However, for the current work, it is more useful to think of Eq. 3 as an additional equation which provides information about the state of the system. Note that $\Delta T_{min} > 0$ in any physically realizable process design.

Now, consider the case of the MHEX model shown in Figure 2. As shown in the figure, we assume that the MHEX operates as an ideal countercurrent exchanger, so that all hot streams are codirectional with each other, and all cold streams are codirectional with each other and oppositely-directed to the hot streams. Beyond this assumption, the internal geometric configuration of the exchanger is not considered in the present work. We also make the common assumption that the heat transfer consequences of fluid dynamics and the material properties of the MHEX can be captured entirely by the overall heat transfer coefficient U. Let the index sets H and C correspond to the hot streams and cold streams involved with the MHEX, respectively. Equation 1 immediately generalizes to the following energy balance:

$$\sum_{i\in H} F_i(T_i^{in}-T_i^{out})=\sum_{j\in C} f_j(t_j^{out}-t_j^{in}). \tag{4}$$

However, the MHEX analogues of Eqs. 2 and 3 are less obvious. Specifically, the concept of the log-mean temperature difference has no immediate generalization to more than two streams, and the minimum temperature difference could occur at the inlet temperature of any stream.

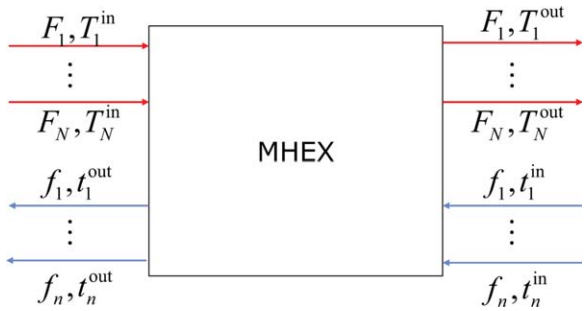

Figure 2. Schematic of a multistream heat exchanger with *N* hot streams and *n* cold streams.

[Color figure can be viewed in the online issue, which is available at wileyonlinelibrary.com.]

Fortunately, the problem of determining the minimum approach temperature in MHEX can be linked to the well-studied field of pinch analysis for heat exchanger networks.

Pinch analysis for heat integration

Pinch analysis is a methodology for minimizing the energy consumption of a chemical process by optimizing heat recovery between process streams. Interpreted graphically, this translates to shifting the process hot and cold composite curves on a temperature-enthalpy (T-Q) graph to maximize their overlap (and hence minimize external utility requirements) while maintaining a certain minimum temperature difference between them (such that a non-negligible thermodynamic driving force exists). The classic formulation of the pinch constraints for simultaneous heat integration and process optimization (due to Duran and Grossmann[7]) is given by

$$\sum_{i\in H} F_i(T_i^{\text{in}}-T_i^{\text{out}})-\sum_{j\in C} f_j(t_j^{\text{out}}-t_j^{\text{in}})+Q_H-Q_C=0, \tag{5}$$

$$AP_C^p-AP_H^p-Q_H\le 0,\quad \forall p\in P, \tag{6}$$

where $P=H\cup C$ is the index set of pinch point candidates, Q_H is the heat load of the heating utilities, Q_C is the heat load of the cooling utilities, and AP_H^p and AP_C^p are defined by

$$AP_H^p=\sum_{i\in H} F_i[\max\{0,T_i^{\text{in}}-T^p\}-\max\{0,T_i^{\text{out}}-T^p\}],\quad \forall p\in P, \tag{7}$$

$$\begin{aligned} AP_C^p=&\sum_{j\in C} f_j[\max\{0,t_j^{\text{out}}-(T^p-\Delta T_{\min})\}\\ &-\max\{0,t_j^{\text{in}}-(T^p-\Delta T_{\min})\}],\quad \forall p\in P. \end{aligned} \tag{8}$$

The temperatures of the pinch point candidates, T^p, are defined by

$$T^p=\begin{cases} T_i^{\text{in}}, & \forall p=i\in H,\\ t_j^{\text{in}}+\Delta T_{\min}, & \forall p=j\in C. \end{cases}$$

As noted in Kamath et al.,[6] a MHEX can be viewed as a special case of a heat exchanger network where the external utilities are not present ($Q_H=0$ and $Q_C=0$), which corresponds graphically to there being complete vertical overlap of the hot and cold composite curves on a T-Q diagram. Under the assumption of maximum heat transfer in a heat exchanger network, it is known that for at least one $p\in P$, the heat deficit constraint (Eq. 6) is active for any feasible set of stream conditions,[7] so the set of inequalities are equivalent to the single equality constraint

$$\max_{p\in P}\{AP_C^p-AP_H^p\}=0. \tag{9}$$

Additionally, the value of $AP_C^p-AP_H^p$ is greater than 0 whenever the heating requirements of the cold streams above the assumed pinch p exceed the available heat content of the hot streams above this temperature level, indicating infeasible heat transfer. The left-hand side of Eq. 9 takes a positive value in this case. Together with the cited result, this implies that the left-hand side of Eq. 9 is always greater than or equal to zero, with equality whenever all heat exchange is feasible. Additionally, due to the nondifferentiability of the $\max\{0,y\}$ function at $y=0$, the following smoothing approximation is often used in practice, which is dependent on a user-defined parameter β[8]:

$$\max\{0,f(x)\}\approx\frac{\left(\sqrt{f(x)^2+\beta^2}+f(x)\right)}{2}. \tag{10}$$

However, an attractive feature of the formulation proposed in this article is that no such approximation is needed; the nondifferentiable nature of the equation system is instead handled directly.

Nonsmooth equation solving and generalized derivative evaluation

Nonsmooth Newton methods are commonly used for solving systems of nonsmooth equations. These methods are used to solve the equation system $\mathbf{f}(\mathbf{y})=\mathbf{0}$ by calculating a sequence of iterates $\{\mathbf{y}^k\}$ starting from an initial guess $\mathbf{y}^0$, where the next iterate is defined by solving the following Newton step for $\mathbf{y}^{k+1}$:

$$\mathbf{G}(\mathbf{y}^k)(\mathbf{y}^{k+1}-\mathbf{y}^k)=-\mathbf{f}(\mathbf{y}^k). \tag{11}$$

Here, $\mathbf{G}(\mathbf{y}^k)$ is a generalized derivative of $\mathbf{f}$ at $\mathbf{y}^k$. When the specific type of generalized derivative evaluated is an element of the B-subdifferential of $\mathbf{f}$ at $\mathbf{y}^k$, the method has the highly desirable property that it converges quadratically in the local neighborhood of the solution, under the additional nontrivial assumption that all elements of the B-subdifferential at the solution are nonsingular.[12] The B-subdifferential is defined as follows.

Definition I. *Let $\mathbf{f}:X\to\mathbb{R}^m$, where X is an open subset of $\mathbb{R}^n$, be a given function that is locally Lipschitz continuous in a neighborhood $N\subset X$ of a vector $\mathbf{x}$. Define the B-subdifferential $\partial_B\mathbf{f}(\mathbf{x})$ to be the nonempty set of limits of sequences $\{\mathbf{Jf}(\mathbf{x}^k)\}$, where each $\mathbf{x}^k\in X$ is a differentiable point of $\mathbf{f}$, $\mathbf{Jf}(\mathbf{x}^k)$ is the Jacobian matrix of $\mathbf{f}$ at $\mathbf{x}^k$, and the sequence $\{\mathbf{x}^k\}$ converges to $\mathbf{x}$. Symbolically,*

$$\begin{aligned} \partial_B\mathbf{f}(\mathbf{x})\equiv\{&\mathbf{H}\in\mathbb{R}^{m\times n}:\mathbf{H}=\lim_{k\to\infty}\mathbf{Jf}(\mathbf{x}^k),\\ &\text{for some sequence }\{\mathbf{x}^k\}\to\mathbf{x},\mathbf{x}^k\notin N_G\}, \end{aligned} \tag{12}$$

where N_G is the set of points of measure zero where $\mathbf{f}$ is not differentiable.

As an example, let $f:\mathbb{R}\to\mathbb{R}$ be defined by $f(x)=|x|$. Then f is only non-differentiable at $x=0$, and the B-subdifferential of f at $x=0$ is given by $\partial_B f(0)=\{-1,1\}$. Elsewhere, the B-subdifferential is a singleton corresponding to the standard derivative. In general though, calculation of elements of the B-subdifferential is highly nontrivial. However, recent advances by Khan and Barton[14] have provided a method for calculating generalized derivatives automatically for certain classes of functions, using an analog of the vector forward mode of automatic differentiation for smooth functions (the reader unfamiliar with the concept of automatic differentiation is referred to the 2008 book by Griewank and Walther[15]). In this work, we focus on automatically calculating generalized derivatives for abs-factorable functions, first defined by Griewank,[16] though the method of Khan and Barton[14] is in fact applicable to an even broader class of functions. We define an abs-factorable function here as a finite composition of absolute value functions and smooth functions. A more rigorous discussion of this class of functions can be found in articles by Khan and Barton[14] and Griewank.[16] Note that the pairwise max and min functions can be expressed in terms of the absolute value function, and as such fall into the category of abs-factorable functions. It is also possible to speak of an algorithm as being

abs-factorable if it can, after unrolling all loops, be represented as an abs-factorable function.[17] This implies several properties about the algorithm, namely, that it does not employ any discontinuous selection (if-else) statements, and that the algorithm must compute the exact same sequence of factors for all inputs of the same data size.

The automatic method of Khan and Barton[14] can evaluate lexicographic directional (LD) derivatives for an abs-factorable function. We forego the precise definition here to keep the exposition clear, and instead say that it is sufficient to think of the LD-derivative as a generalization of the classical directional derivative which is resolved in a sequence of p directions, instead of a single direction. For a function $\mathbf{f} : X \subset \mathbb{R}^n \to \mathbb{R}^m$ with X open, the LD-derivative of $\mathbf{f}$ at a vector $\mathbf{x} \in X$ in the directions $\mathbf{M} \in \mathbb{R}^{n\times p}$ is denoted by $\mathbf{f}'(\mathbf{x};\mathbf{M}) \in \mathbb{R}^{m\times p}$. In this work, the matrix $\mathbf{M}$ of directions will usually be taken as the $n \times n$ identity matrix $\mathbf{I}$. Of particular interest for this work is the fact that the LD-derivative of an abs-factorable function in the directions $\mathbf{I}$ is also guaranteed to be an element of that function's B-subdifferential.[14] This implies that we can achieve local quadratic convergence to a solution of a nonsmooth equation system using nonsmooth Newton methods that employ automatically calculated LD-derivatives as the generalized derivative information.

Formulation of MHEX Minimum Approach Temperature Constraint

To enforce feasible heat transfer in MHEX, we will use a variant of Eq. 9 in the model. However, we do not wish to use Eqs. 4 and 9 directly in an equation solving procedure because the system will usually have a nonunique solution; there are many sets of stream conditions that give feasible heat transfer for a MHEX in energy balance. While there are nonsmooth equation solving methods that can tolerate nonuniqueness (one of which is discussed further later), the single solution that is returned becomes dependent on the initial guess provided to the solver.

Instead, we wish to formulate the problem so that its only solution is the one corresponding to the minimum temperature difference between hot and cold streams in the MHEX being exactly $\Delta T_{\min}$. A solution of this form maximizes the heat transferred in the MHEX. Geometrically, this is the problem of attempting to reduce the smallest vertical separation between the hot and cold composite curves to exactly $\Delta T_{\min}$. This is equivalent to the problem of reducing the smallest horizontal distance between the composite curves to zero after applying a temperature shift of $\Delta T_{\min}$ to the cold curve.

To obtain functions which describe the shape of the composite curves, we reverse the order of the temperature terms inside the max statements of AP_H^p and AP_C^p and take the negative of the expressions. We are therefore accounting for heat transfer below, rather than above, the pinch. We also note that both curves are not defined at every temperature, and so the horizontal distance could be undefined at certain points. This can be solved by creating nonphysical extensions of the curves which extend to the maximum and minimum temperatures existing in the heat exchanger by adding additional terms. With these modifications, the hot and cold composite curve enthalpy values corresponding to each pinch point temperature are defined using the following expressions:

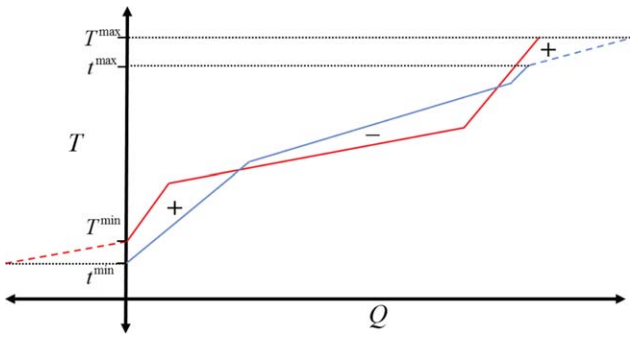

Figure 3. Illustration of the extended composite curves generated by the expressions EBP_C^p (blue) and EBP_H^p (red) when P is expanded to include both inlet and outlet temperatures.

The dashed lines indicate the extended portions of the curves added by the last two terms in Eqs. 13 and 14. The sign of $EBP_C^p - EBP_H^p$ is indicated in the various regions of the plot. [Color figure can be viewed in the online issue, which is available at wileyonlinelibrary.com.]

$$EBP_H^p = \sum_{i\in H} F_i[\max\{0, T^p - T_i^{\text{out}}\} - \max\{0, T^p - T_i^{\text{in}}\} - \max\{0, T^{\min} - T^p\} + \max\{0, T^p - T^{\max}\}], \forall p \in P, \tag{13}$$

$$EBP_C^p = \sum_{j\in C} f_j[\max\{0, (T^p - \Delta T_{\min}) - t_j^{\text{in}}\} - \max\{0, (T^p - \Delta T_{\min}) - t_j^{\text{out}}\} + \max\{0, (T^p - \Delta T_{\min}) - t^{\max}\} - \max\{0, t^{\min} - (T^p - \Delta T_{\min})\}], \forall p \in P, \tag{14}$$

where $T^{\max}$ is the maximum hot stream inlet temperature, $T^{\min}$ is the minimum hot stream outlet temperature, $t^{\max}$ is the maximum cold stream outlet temperature, and $t^{\min}$ is the minimum cold stream inlet temperature. In each equation, the last two terms correspond to the nonphysical extensions of the curves. We also note that whenever one of these additional terms is nonzero in Eq. 13, it will be multiplied by the sum of all the hot stream heat capacity flowrates, and similarly for Eq. 14 with the sum of the cold stream heat capacity flowrates. Figure 3 shows the full extended composite curves generated by evaluating Eqs. 13 and 14 for an example set of inlet and outlet temperatures for a MHEX. In practice however, the expressions need only be evaluated at the known pinch candidate temperatures. We also note that it is entirely possible to transform Eqs. 13 and 14 into expressions which preserve the order of terms and signs in Eqs. 7 and 8, however, the geometric interpretation for the form of the extensions is less obvious in this formulation.

The smallest horizontal distance between the extended composite curves can now be found by solving

$$\min_{p\in P}\{EBP_C^p - EBP_H^p\} = 0. \tag{15}$$

It can also be seen that the expression inside the min statement of Eq. 15 is negative at any pinch temperature where the hot composite curve lies to the right of the shifted cold composite curve, and positive where it lies to the left, as indicated in Figure 3. After calculating $EBP_C^p - EBP_H^p, \forall p \in P$, we solve Eq. 15 by searching through the finite set P to find the minimum. This can be done using an abs-factorable algorithm in analogy to Algorithm 6.1 in Khan and Barton[17] (first computing $T^{\max}, T^{\min}, t^{\max}, t^{\min}$ and then evaluating Eqs. 13, 14, and 15 in place of Eqs. 7, 8, 9). As such, generalized derivatives

Table 1. Stream Data for Example 1

Stream Name	T^{in} or t^{in} (°C)	T^{out} or t^{out} (°C)	F or f (MW°C^{-1})
H1	250	40	0.15
H2	200	y_1	0.25
C1	20	180	0.20
C2	140	y_2	0.30

can be calculated automatically for Eq. 15 with respect to the unknown variables. We now present a small example to examine the method thus far and highlight an additional issue with the solution process.

Example I. *Consider the process data in Table* 1 *for two hot streams and two cold streams in a* MHEX *(adapted from a heat exchanger network example in Smith*[18]*).*

Let $\Delta T_{\min} = 10$°C for this example. The equation system that must be solved for the unknown temperatures $y_1 \equiv T_{H2}^{out}$ and $y_2 \equiv t_{C2}^{out}$ consists of Eqs. 4 and 15. For the solution to be feasible, we must also have that $T_i^{out} \leq T_i^{in}, \forall i \in H$ and $t_j^{out} \geq t_j^{in}, \forall j \in C$. When modeling a MHEX using this formulation, it is recommended that one unknown correspond to a hot stream outlet and the other correspond to a cold stream outlet, as is the case here. Figure 4 shows the residual functions for Eqs. 4 and 15 plotted for a range of y_1 and y_2 values around the solution.

The system is clearly nonsmooth, and so we apply Eq. 11 iteratively to the problem from the initial guess $\mathbf{y}^0 = (80, 230)$, the solution from Smith[18] with utilities present. We use the infinity norm of the residual functions as the basis for termination; here we consider the problem to have converged when the value is less than 10^{-9}. The solution corresponding to the MHEX which maximizes heat transfer is found after just a single iteration to be $\hat{\mathbf{y}} = (120, 205)$. The (non-extended) composite curves at the solution are shown in Figure 5. Figure 6 shows the zero-level contours of Eqs. 4, 9, and 15 applied to this example over a range of values for $\mathbf{y}$. We note that the solution is unique using the proposed formulation, but that there are infinitely many solutions if we use Eq. 9 in place of Eq. 15, since its residual is zero over a large region that partially overlaps with the zero-level contour of the energy balance residual. Note that both of these formulations will have flat regions in the residual plots; such regions are a natural feature of the MHEX problem because unknowns such as inlet and outlet temperatures will only influence the minimum distance between the composite curves over limited ranges of values. However, the extensions we have defined have the effect of moving this flat region to a nonzero residual function value, which eliminates the nonuniqueness of the solution in many cases.

We also note that if a nonsmooth Newton method is started from any point with $y_1 > 130$, where the surface corresponding to Eq. 15 is flat, the method fails to solve the Newton step for the next iterate because the generalized derivative is a singleton corresponding to the standard Jacobian matrix, which is singular.

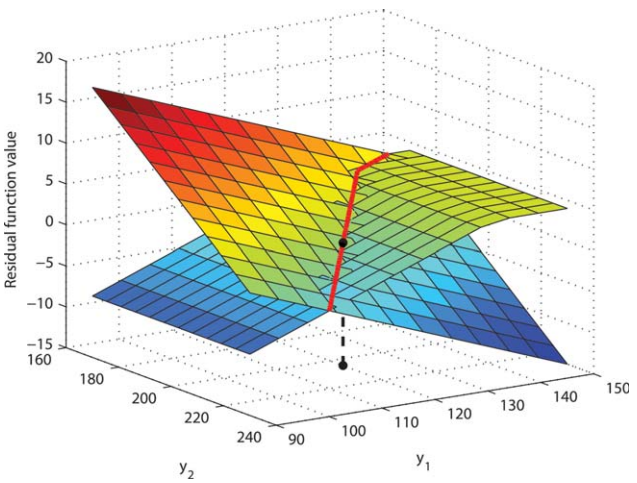

Figure 4. Equation system in the vicinity of the solution for Example 1.

The intersection of the two surfaces is indicated by the solid line. The solution point is shown both on the surfaces and projected onto the y_1-y_2 plane. [Color figure can be viewed in the online issue, which is available at wileyonlinelibrary.com.]

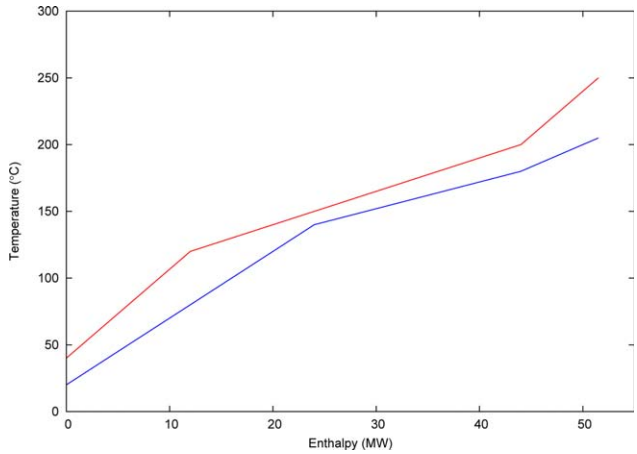

Figure 5. The composite curves corresponding to the multistream heat exchanger simulated in Example 1.

[Color figure can be viewed in the online issue, which is available at wileyonlinelibrary.com.]

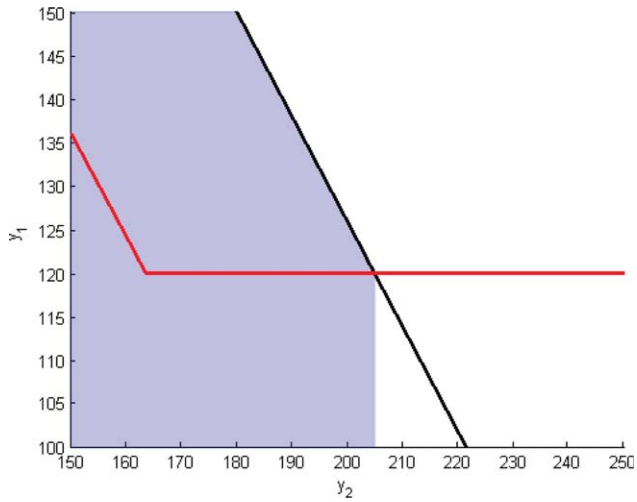

Figure 6. Zero-level contours for Eqs. 4 (black line), 9 (shaded region), and 15 (red line) for the problem in Example 1 over a range of values for the unknown temperatures.

[Color figure can be viewed in the online issue, which is available at wileyonlinelibrary.com.]

As a result of the unavoidable presence of singular Jacobians, the nonsmooth Newton method based on Eq. 11 cannot solve the problem starting from any possible initial guess. Recently, Facchinei et al.[13] developed a linear program (LP) based Newton method that works for nonsmooth equation systems and does not require nonsingularity of generalized derivative elements. At each step, this method solves the following LP for the next iterate:

$$\begin{aligned} &\min_{\gamma,\mathbf{y}} \ \gamma \\ &\text{s.t.} \|\mathbf{f}(\mathbf{y}^k)+\mathbf{G}(\mathbf{y}^k)(\mathbf{y}-\mathbf{y}^k)\|_\infty \le \gamma\|\mathbf{f}(\mathbf{y}^k)\|_\infty^2, \\ &\|(\mathbf{y}-\mathbf{y}^k)\|_\infty \le \gamma\|\mathbf{f}(\mathbf{y}^k)\|_\infty, \\ &\gamma \ge 0, \\ &\mathbf{y} \in Y. \end{aligned} \tag{16}$$

In practice, the infinity norms are replaced by their equivalent linear reformulations. This method is well suited for the problem at hand. In addition to not failing when given a singular generalized derivative element, the method achieves local Q-quadratic convergence when an element of the B-subdifferential is used for $\mathbf{G}(\mathbf{y}^k)$, and allows for known polyhedral bounds (expressed as the set Y) on $\mathbf{y}$ to be included in the LP. As an example, a useful bound that could be added when $\Delta T_{\min}$ is an unknown is $\Delta T_{\min} \ge \Delta T_{\text{tol}}$, where $\Delta T_{\text{tol}} > 0$ is the smallest approach temperature that would be tolerated in operation. The bounds on the unknown temperatures should also be enforced, for instance, if some y_k corresponds to a hot stream outlet temperature T_i^{out} for some i, then we add the constraint $y_k \le T_i^{\text{in}}$. This prevents the hot stream from gaining heat as if it were a cold stream, which would invalidate the model. Analogous constraints can be imposed for variables corresponding to inlet or cold stream temperatures. Using the LP-Newton method on the problem given in Example 1 gives the correct solution regardless of whether or not the Jacobian is singular at the initial guess, although the method is no longer exact for linear equations as the previous method was, so the number of iterations needed to converge is greater (around 40 iterations were needed for all initial guesses tested).

Formulation of MHEX Area Constraint

Consider now an analogue of Eq. 2 for the MHEX case. Define K as the index set for the points at which the composite curves are nondifferentiable (kinks), as well as their endpoints, then for $k \in K$, let Q^k denote the enthalpy value at this kink or endpoint, which could occur on either the hot or cold composite curve. Now suppose we have a list of triples of the form (Q^k, T^k, t^k), ordered by nondecreasing Q^k value. For each of these triples, T^k is the temperature on the hot composite curve at Q^k, and t^k is the temperature on the cold composite curve at Q^k. An adjacent pair of triples in the list demarcates an interval of the composite curves in which part of MHEX can be modeled as a two-stream heat exchanger. A simple expression for the total required heat transfer area of a network of two-stream heat exchangers which can be applied to MHEX is as follows[18,19]:

$$UA = \sum_{\substack{k \in K \\ k \ne |K|}} \frac{\Delta Q^k}{\Delta T_{\text{LM}}^k}, \tag{17}$$

where $\Delta Q^k = Q^{k+1} - Q^k$ is the width of enthalpy interval k, $|K| = 2(|H|+|C|)$, and ΔT_{LM}^k is a modified version of the log-mean temperature difference across this same enthalpy interval which is defined later in this section. Figure 7 illustrates

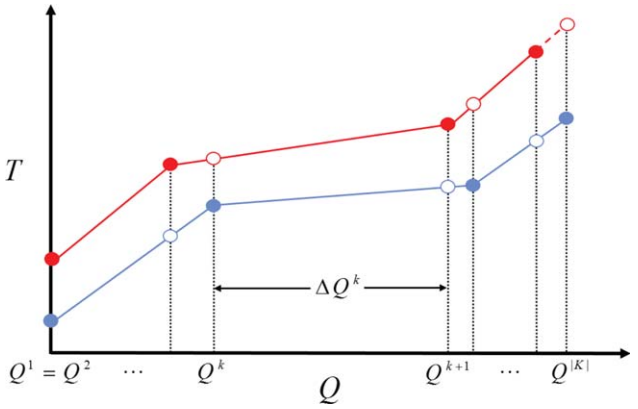

Figure 7. Example of the enthalpy intervals used in the calculation of Eq. 17.

Solid circles represent the temperatures which are part of the data for the problem, hollow circles represent those which must be calculated. In the case where the endpoints of the composite curves do not align, one curve must be extrapolated out to the end of the other (dashed line). [Color figure can be viewed in the online issue, which is available at wileyonlinelibrary.com.]

the definitions of Q^k and ΔQ^k for a sample set of composite curves. Note that for this work, we assume that there can be no transverse heat transfer between adjacent enthalpy intervals.

In standard practice, heat transfer area is calculated after heat integration is performed, and the the integrated composite curves are used to define the enthalpy intervals. However, in this work, we wish to include Eq. 17 in the system of equations being solved simultaneously, so that we have an additional unknown for simulation and the area is specified as part of the problem input. This creates some difficulty, as we must calculate the full sorted list of (Q^k, T^k, t^k) triples at each iteration, starting from an incomplete list of just the inlet and outlet temperatures which are arranged in an arbitrary order. Furthermore, this must be done using an algorithm for which we can calculate valid generalized derivatives.

We begin by arbitrarily ordering the set of inlet and outlet temperatures into a list indexed by a set L of size $|K|$. Then for each $l \in L$, we calculate the pre-sort enthalpy P^l using one of the following equations:

$$\begin{aligned} &P^l = \sum_{i \in H} F_i\left(\max\{0, T^l - T_i^{\text{out}}\} - \max\{0, T^l - T_i^{\text{in}}\}\right), \\ &T^l \in \{T_i^{\text{in/out}} : i \in H\}, \end{aligned} \tag{18}$$

$$\begin{aligned} &P^l = \sum_{j \in C} f_j\left(\max\{0, t^l - t_j^{\text{in}}\} - \max\{0, t^l - t_j^{\text{out}}\}\right), \\ &t^l \in \{t_j^{\text{in/out}} : j \in C\}. \end{aligned} \tag{19}$$

This provides all the enthalpy values we need to calculate the heat transfer area, but they are out of order and not yet associated with the corresponding pair of temperatures on the composite curves. To correct the order, we create a list of triples, each of the form (P^l, T^l, t^l), in which each P^l is associated with either the hot or cold temperature used in its calculation (and as such one of the temperature entries is currently unknown in each triple). We then sort this list into nondecreasing order based on enthalpy value to set up the intervals for Eq. 17 correctly. If the sort is performed using a naïve bubble sort, implemented as shown in Figure 8, then the only

Input : An unsorted list, A with entries $A[1],\ldots,A[m]$.
Output: The list A, with the m entries sorted in order of increasing value.

for $i \leftarrow 1$ **to** m **do**
  for $j \leftarrow 1$ **to** $m-1$ **do**
    $a \leftarrow \min(A[j],A[j+1])$
    $b \leftarrow \max(A[j],A[j+1])$
    $A[j] \leftarrow a$
    $A[j+1] \leftarrow b$
return A

Figure 8. The naïve bubble sort algorithm.

operations involve taking the max or min of two values. The loops are run over the entire length of the list to ensure that the same number of operations are performed for a given input size, regardless of how well-sorted the input data is. These conditions imply that the sort algorithm has an abs-factorable representation and therefore has well-defined LD-derivatives which can be calculated automatically. We therefore view the sorting operation as a nonsmooth function which maps the unsorted input to the sorted output. As shown in Khan and Barton,[14] LD-derivatives obey a sharp chain rule, so by evaluating the LD-derivatives of the sorting function in the directions set by the LD-derivatives of the inner function which maps $\mathbf{y}$ to the list of P^l values, as given in Eqs. 18 and 19, we obtain valid LD-derivatives of the composite function in the original directions $\mathbf{I}$. Example 2 demonstrates this initial part of the procedure.

Example 2. *Consider the stream data from the previous example at the solution point* $\hat{\mathbf{y}}$. *We begin by calculating the enthalpy values and their LD-derivatives at* $\hat{\mathbf{y}}$ *in the directions* $\mathbf{I}$. *This is performed in the C++ programming language using the implementation of automatic LD-derivative evaluation described in Khan and Barton.*[14] *Table* 2 *contains these values for this example.*

We arrange this data into triples of the form (P^l, T^l, t^l) and apply the bubble sort algorithm to sort by nondecreasing enthalpy value. The result of this operation is the list of correctly ordered but incomplete triples as shown in Table 3.

We note that here, the LD-derivatives associated with each P^l prior to the sort remain associated with the corresponding variable in the sorted order. In general, however, this need not be the case. For instance, if for $l=1$, we instead had $P^{l'}(\hat{\mathbf{y}};\mathbf{I})=[0.25\ 0]$, then following the sort, the ordering of triples is identical, but $Q^{7'}(\hat{\mathbf{y}};\mathbf{I})=[0\ 0.3]$, and $Q^{8'}(\hat{\mathbf{y}};\mathbf{I})=[0.25\ 0]$.

Now we must calculate the missing temperature in each of the triples. Given Q^k, if T^k is unknown, we must solve Eq. 20 for T^k. Similarly, if t^k is unknown, then we must solve Eq. 21 for t^k:

Table 2. Temperature-Enthalpy Data for the Streams in Example 1

l	Temperature ID	Temperature (°C)	$P^l(\hat{\mathbf{y}})$(MW)	$P^{l'}(\hat{\mathbf{y}};\mathbf{I})$
1	T_1^{in}	250	51.5	[−0.25 0]
2	T_1^{out}	40	0.0	[0 0]
3	T_2^{in}	200	44.0	[−0.25 0]
4	T_2^{out}	120	12.0	[0.15 0]
5	t_1^{in}	20	0.0	[0 0]
6	t_1^{out}	180	44.0	[0 0]
7	t_2^{in}	140	24.0	[0 0]
8	t_2^{out}	205	51.5	[0 0.3]

Table 3. Results of the Bubble Sort Operation on the Triples Generated from Table 2

k	$(Q^k(\hat{\mathbf{y}}), T^k, t^k)$	$Q^{k'}(\hat{\mathbf{y}};\mathbf{I})$
1	(0, 40, –)	[0 0]
2	(0, –, 20)	[0 0]
3	(12, 120, –)	[0.15 0]
4	(24, –, 140)	[0 0]
5	(44, 200, –)	[−0.25 0]
6	(44, – 180)	[0 0]
7	(51.5, 250, –)	[−0.25 0]
8	(51.5, –, 205)	[0 0.3]

The symbol "-" represents those temperatures which have yet to be calculated.

$$Q^k-\sum_{i\in H}F_i\left(\max\{0,T^k-T_i^{\text{out}}\}-\max\{0,T^k-T_i^{\text{in}}\}\right)=0, \quad (20)$$

$$Q^k-\sum_{j\in C}f_j\left(\max\{0,t^k-t_j^{\text{in}}\}-\max\{0,t^k-t_j^{\text{out}}\}\right)=0. \quad (21)$$

Unfortunately, there seems to be no way to solve either of these equations for the unknown temperature without the use of selection statements, and so any such algorithm would not have an abs-factorable representation. Therefore, since we cannot guarantee that valid B-subdifferential elements would be obtained by differentiating the solution algorithm, we must proceed by a different method.

If no restrictions are placed on the algorithm, the value of the unknown temperature, denoted by $\hat{T}^k$ or $\hat{t}^k$, that satisfies Eqs. 20 or 21 can be determined by a simple search and interpolation procedure over the piecewise affine segments of the relevant composite curve. As shown in Figure 7, if the composite curves do not exactly align, the shorter curve can be extrapolated to the end of the longer one to find the corresponding temperature.

We then need to calculate independently the LD-derivatives of this temperature at the value of the vector of unknowns, $\hat{\mathbf{y}}$, in the original directions $\mathbf{I}$, for example, $T^{k'}(\hat{\mathbf{y}};\mathbf{I})$ or $t^{k'}(\hat{\mathbf{y}};\mathbf{I})$. However, we cannot do this directly, so instead we think of Eq. 20 (and analogously Eq. 21) as $h(T^k,\mathbf{y},Q^k(\mathbf{y}))=0$, for the function $h:\mathbb{R}\times\mathbb{R}^{n_y}\times\mathbb{R}\rightarrow\mathbb{R}$ defined by the left-hand side of Eq. 20. Therefore, we have an implicit function $\eta:\mathbb{R}^{n_y}\times\mathbb{R}\rightarrow\mathbb{R}$ defined by the equation $h(T^k,\mathbf{y},Q^k(\mathbf{y}))=0$, such that $T^k(\mathbf{y})=\eta(\mathbf{y},Q^k(\mathbf{y}))$, for all $\mathbf{y}$ in a neighborhood of $\hat{\mathbf{y}}$. We note that the implicit function here depends on Q^k which is (possibly) a function of the unknowns $\mathbf{y}$, so we apply the chain rule to obtain the desired LD-derivatives $T^{k'}(\hat{\mathbf{y}};\mathbf{I})=\eta'((\hat{\mathbf{y}},Q^k(\hat{\mathbf{y}}));\mathbf{M})$, where the directions $\mathbf{M}$ are determined by the LD-derivatives of the previous operations which calculated $Q^k(\hat{\mathbf{y}})$. To calculate the LD-derivatives $\eta'((\hat{\mathbf{y}},Q^k(\hat{\mathbf{y}}));\mathbf{M})$ correctly, we invoke the lexicographic implicit function theorem from Khan.[20] The form of the lexicographic implicit function theorem suggests an algorithm for calculating this derivative, based on searching through the family $\mathscr{F}_h$ of continuously differentiable selection functions ϕ which comprise the piecewise continuously-differentiable function h. The correctness of this algorithm was proven by Khan,[20] and the algorithm itself is reproduced in Figure 9 here.

The computational complexity of this algorithm applied naïvely is exponential in the number of hot and cold streams because of the presence of $4^{|H|}$ selection functions due to the binary max terms in the definition of h, where each term has two possible differentiable functional forms that could be active at $h(\hat{T}^k,\hat{\mathbf{y}},Q^k(\hat{\mathbf{y}}))$. However, this unfavorable scaling

forall the $\phi \in \mathcal{F}_{\mathbf{h}}(\hat{\mathbf{x}},\hat{\mathbf{z}})$ **do**
  if $\frac{\partial \phi}{\partial \mathbf{x}}(\hat{\mathbf{x}},\hat{\mathbf{z}})$ *is nonsingular* **then**
    Solve the linear equation system $\frac{\partial \phi}{\partial \mathbf{x}}(\hat{\mathbf{x}},\hat{\mathbf{z}})\mathbf{A} = -\frac{\partial \phi}{\partial \mathbf{z}}(\hat{\mathbf{x}},\hat{\mathbf{z}})\mathbf{M}$ for $\mathbf{A} \in \mathbb{R}^{m\times p}$
    if $\mathbf{h}'((\hat{\mathbf{x}},\hat{\mathbf{z}});(\mathbf{A},\mathbf{M})) = \mathbf{0}_{m\times p}$ **then**
      return $\boldsymbol{\eta}'(\hat{\mathbf{z}};\mathbf{M}) := \mathbf{A}$

Figure 9. Algorithm for the calculation of LD-derivatives $\boldsymbol{\eta}'(\hat{\boldsymbol{z}};\mathbf{M})$ for a function $\boldsymbol{\eta}$ implicitly defined by the equation $\mathbf{h}(\boldsymbol{\eta}(\mathbf{z}),\mathbf{z})=\mathbf{0}$ such that $\hat{\mathbf{x}}=\boldsymbol{\eta}(\hat{\mathbf{z}})$.

can be mitigated by using the calculated value of the unknown temperature itself to reduce the number of possible active selection functions. Once the value and the corresponding LD-derivative of the unknown temperature have been calculated, they are copied into the appropriate object type and used in the remainder of the procedure. Example 3 demonstrates the application of the lexicographic implicit function theorem.

Example 3. *Consider the triples from the previous example. A kink in the cold composite curve is located at* $\hat{Q}^k = 44$ *MW, corresponding to a cold stream temperature value of* $\hat{t}^k = 180°C$. *We notice that here, the hot temperature value is actually already known at this enthalpy value, so* $\hat{T}^k = 200°C$ *(if this was not the case, we could interpolate on the relevant affine segment to find* $\hat{T}^k$*). Note that the LD-derivatives (and regular derivatives) of* Q^k *at this* $\hat{\mathbf{y}}$ *are all zero, since the value of the cold stream outlet variable* $\hat{y}_2 = 205°C$ *is strictly greater than all other cold stream temperatures, and so Eq. 21 shows that only the zero selection function of the max term involving* $y_2 \equiv t_2^{out}$ *will be active when* $\hat{t} = 180°C$. *For notational consistency with the algorithm in Figure 9, define* $\mathbf{z}(\mathbf{y}) = (\mathbf{y}, Q^k(\mathbf{y}))$*, and then the direction matrix* $\mathbf{M}$ *is given by*

$$\mathbf{M} = \begin{bmatrix} \mathbf{I} \\ Q^{k'}(\hat{\mathbf{y}};\mathbf{I}) \end{bmatrix} = \begin{bmatrix} 1 & 0 \\ 0 & 1 \\ 0 & 0 \end{bmatrix}.$$

Then we can write Eq. 20 for this example as follows:

$$h(T^k,\mathbf{z}) = z_3 - F_1\left(\max\{0, T^k - T_1^{\text{out}}\} - \max\{0, T^k - T_1^{\text{in}}\}\right) - F_2\left(\max\{0, T^k - z_1\} - \max\{0, T^k - T_2^{\text{in}}\}\right) = 0.$$

Naïvely, we would need to consider 16 different continuous selection functions here to account for the four max terms; however, we note that three of the max terms will only have a single active selection function, since $\hat{T}^k > T_1^{\text{out}}$, $\hat{T}^k < T_1^{\text{in}}$, and $\hat{T}^k > \hat{z}_1$. In the final term however, $\hat{T}^k = T_2^{\text{in}}$, so we will have two possible differentiable selection functions to consider: $\phi_1, \phi_2 \in \mathcal{F}_h(\hat{T}^k,\hat{\mathbf{z}})$, where

$$\phi_1(T^k,\mathbf{z}) = z_3 - F_1\left(T^k - T_1^{\text{out}}\right) - F_2\left(T^k - z_1\right),$$
$$\phi_2(T^k,\mathbf{z}) = z_3 - F_1\left(T^k - T_1^{\text{out}}\right) - F_2\left(T^k - z_1\right) + F_2\left(T^k - T_2^{\text{in}}\right).$$

Evaluating the required derivatives gives

$$\frac{\partial \phi_1}{\partial \mathbf{z}}(\hat{T}^k,\hat{\mathbf{z}}) = [F_2\ 0\ 1], \quad \frac{\partial \phi_2}{\partial \mathbf{z}}(\hat{T}^k,\hat{\mathbf{z}}) = [F_2\ 0\ 1],$$
$$\frac{\partial \phi_1}{\partial T^k}(\hat{T}^k,\hat{\mathbf{z}}) = -(F_1+F_2), \quad \frac{\partial \phi_2}{\partial T^k}(\hat{T}^k,\hat{\mathbf{z}}) = -F_1.$$

In practical implementation of this algorithm, these expressions can all be calculated using automatic differentiation. Solving the linear system $\frac{\partial \phi_1}{\partial T^k}(\hat{T}^k,\hat{\mathbf{z}})\boldsymbol{A}_1 = -\frac{\partial \phi_1}{\partial \mathbf{z}}(\hat{T}^k,\hat{\mathbf{z}})\mathbf{M}$ for $\boldsymbol{A}_1$ then yields $\boldsymbol{A}_1 = [\frac{F_2}{F_1+F_2}\ 0] = [0.625\ 0]$. However, evaluation of the LD-derivative of h yields $h'((\hat{T}^k,\hat{\mathbf{z}});(\boldsymbol{A}_1,\mathbf{M})) = [0.15625\ 0]$, indicating that $\eta'(\hat{\mathbf{z}};\mathbf{M}) \neq \boldsymbol{A}_1$. Solving the linear system involving ϕ_2 gives $\boldsymbol{A}_2 = [\frac{F_2}{F_1}\ 0] = [\frac{5}{3}\ 0]$. In this case, evaluation of the LD-derivative of h yields $h'((\hat{T}^k,\hat{\mathbf{z}});(\boldsymbol{A}_2,\mathbf{M})) = [0\ 0]$, and so $\eta'(\hat{\mathbf{z}};\mathbf{M}) = \boldsymbol{A}_2$ Finally, by the chain rule for LD-derivatives, we have that

$$T^{k'}(\hat{\mathbf{y}};\mathbf{I}) = \eta'\left((\hat{\mathbf{y}}, Q^k(\hat{\mathbf{y}})); \begin{bmatrix} \mathbf{I} \\ Q^{k'}(\hat{\mathbf{y}};\mathbf{I}) \end{bmatrix}\right) = \eta'(\mathbf{z}(\hat{\mathbf{y}});\mathbf{M}) = \boldsymbol{A}_2.$$

Applying this procedure for all Q^k, we complete the sorted list of triples at all nondifferentiable points on the composite curves. Now we must calculate the log-mean temperature difference between the endpoints of each enthalpy interval. To do this, it is necessary to slightly alter the standard definition of the log-mean temperature difference so that evaluating the function never results in undefined behavior. The definition used for this work is as follows (from Zavala-Río et al.[21]):

$$\Delta T_{\text{LM}}^k(\Delta T^k, \Delta T^{k+1}) = \begin{cases} \frac{1}{2}(\Delta T^k + \Delta T^{k+1}) & \text{if } \Delta T^k = \Delta T^{k+1}, \\ \frac{\Delta T^{k+1} - \Delta T^k}{\ln(\Delta T^{k+1}) - \ln(\Delta T^k)} & \text{otherwise,} \end{cases} \tag{22}$$

where $\Delta T^k = \max\{\Delta T_{\min}, T^k - t^k\}$ is the temperature difference at the start of enthalpy interval k, and $\Delta T^{k+1} = \max\{\Delta T_{\min}, T^{k+1} - t^{k+1}\}$ is the temperature difference at the end of the interval. We take the max with $\Delta T_{\min}$ here so that this calculation of the temperature driving force is only based on feasible heat transfer. The if statement in the definition of the log-mean temperature difference is necessary to make the calculation defined for all possible inputs $\Delta T^k > 0$ and $\Delta T^{k+1} > 0$. Fortunately, since this function is continuously differentiable on the positive quadrant of $\mathbb{R}^2$, [21] the if statement in Eq. 22 does not introduce any complications since the standard rules for automatic differentiation will produce correct derivatives. We note that the function obtained by composing the function $T^k(\mathbf{y})$ (which is itself already a composition of several nonsmooth functions) with the max functions defining ΔT^k and ΔT^{k+1}, and then the log-mean temperature difference function remains a nonsmooth function of the unknowns $\mathbf{y}$. As before, we note that we able to calculate the correct LD-derivatives of this composite function through application of the chain rule.

In summary, the set of equations describing the MHEX now consists of the following:

$$\sum_{i\in H} F_i(T_i^{\text{in}} - T_i^{\text{out}}) - \sum_{j\in C} f_j(t_j^{\text{out}} - t_j^{\text{in}}) = 0,$$
$$\min_{p\in P}\{EBP_H^p - EBP_C^p\} = 0,$$
$$UA - \sum_{\substack{k\in K \\ k\neq |K|}} \frac{\Delta Q^k}{\Delta T_{\text{LM}}^k} = 0.$$

This is a nonsmooth equation system involving three equations in three unknowns which can solved using the LP-Newton method discussed previously. Additionally, we must ensure that $T_i^{\text{out}} \leq T_i^{\text{in}}, \forall i \in H$ and $t_j^{\text{out}} \geq t_j^{\text{in}}, \forall j \in C$, which is most easily enforced by setting polyhedral bound constraints

Table 4. Stream Data for Example 4

Stream Name	T^{in} or t^{in} (°C)	T^{out} or t^{out} (°C)	F or f (kW°C^{-1})
H1	160.0	93.3	8.8
H2	248.9	137.8	10.6
H3	226.7	65.6	14.8
H4	271.1	148.9	12.6
H5	198.9	65.6	17.7
C1	60.0	160.0	7.6
C2	115.6	221.7	6.1
C3	37.8	221.1	8.4
C4	82.2	176.7	17.3
C5	93.3	204.4	13.9

in the LP-Newton method. We also note that since it is necessary to calculate the temperature difference between the composite curves at each Q^k in order to evaluate Eq. 17, one can use the following in place of Eq. 15 in the previous equation system

$$\min_{k\in K}\{T^k-(t^k+\Delta T_{\min})\}=0. \tag{23}$$

This is a more expensive function to evaluate than Eq. 15, although since most of the computational work must be done to evaluate Eq. 17, using it in the system of three equations will be slightly cheaper computationally overall. Our testing has not been conclusive as to which of these two possible formulations results in faster convergence to the solution; it appears largely dependent on the problem at hand and the initial guess provided.

A larger illustrative example that makes use of the full MHEX model is now given.

Example 4. *Consider the following process data in Table* 4 *for five hot streams and five cold streams in a* MHEX *(adapted from a heat exchanger network example in Chakraborty and Ghosh*[22]*). We simulate this MHEX under four different conditions to highlight the flexibility of our model. In all cases, we use the CPLEX v12.5 callable library*[23] *to solve the* LP *at each iteration. We consider the problem to have converged to a solution when the infinity norm of the residual functions is less than* 10^{-9}.

Case I. *For a first example, let* $y_1 \equiv T^{out}_{H5}$, $y_2 \equiv t^{out}_{C5}$, *and* $y_3 \equiv UA$. *Let all other temperatures be fixed at their values in Table* 4 *and let* $\Delta T_{\min}=10$°C. *Solving the system of three equations (*4, 15, and 17*) using the LP-Newton method yields* $y_1=131.3$°C, $y_2=259.0$°C, *and* $y_3=314.7$ kW/K *after 125 iterations starting from the solution with utilities present given by Chakraborty and Ghosh*[22] *and* $y^0_3=200$ kW/K. *The composite curves for the* MHEX *in this case are shown in* Figure 10a. *We make the observation that the composite curves resemble those of a two-stream heat exchanger involving streams of nonconstant heat capacity, despite actually consisting of a number of affine segments. The same numerical result is obtained by applying only* Eqs. 4 *and* 15 *to resolve the composite curves and then calculating UA afterward.*

Case II. *The strength of the new approach is more apparent when UA is specified, rather than calculated. Given UA, a typical problem is to calculate* $\Delta T_{\min}$ *in the exchanger, which generally leads to better design than when* $\Delta T_{\min}$ *is specified*[24] *(as it was in Case I). For a second example, assume that we are re-purposing an old heat exchanger with a* $UA=400$kW/K, *let* $y_1 \equiv T^{out}_{H5}$, $y_2 \equiv t^{out}_{C5}$ *as before, and now let* $y_3 \equiv \Delta T_{\min}$. *Starting from the conditions at the solution of the previous case, the new solution is found in 13 iterations of the LP-Newton method with* $y_1=126.2$°C, $y_2=265.5$°C, *and* $y_3=3.5$°C. *The composite curves for the* MHEX *in this case are shown in* Figure 10b. *Here, the curves are more closely pinched together than in Case I as a result of the increased heat transfer potential afforded by the higher UA value.*

Case III. *Now consider using the same variables as in Case II, but using a heat exchanger instead with* $UA=200$ kW/K. *The solution is found in 49 iterations of the LP-Newton method with* $y_1=162.4$°C, $y_2=219.4$°C, *and* $y_3=16.7$°C *starting from the conditions at the solution of Case I. The composite curves for the* MHEX *in this case are shown in* Figure 10c. *In this case, we see the location of the pinch shifts to a significantly lower temperature than in Cases I and II. We also see* T^{out}_{H5} *increase and* t^{out}_{C5} *decrease substantially in response to the decrease in UA, resulting in a larger temperature gap between the composite curves than in the previous cases.*

Case IV. *Finally, consider the problem where* $y_1 \equiv T^{out}_{H5}$, $y_2 \equiv t^{out}_{C5}$, *and* y_3 *is a third temperature, say* $y_3 \equiv T^{out}_{H1}$, *with* $\Delta T_{min}=10°C$. *We must also specify a value of* UA *for this MHEX, though we note that not all values of* UA *will lead to a feasible solution due to the highly constrained nature of the problem. If we let* $UA=340kW/K$, *then the solution is found in 26 iterations with* $y_1=140.1°C$, $y_2=259.0°C$, *and* $y_3=75.6°C$ *starting from the conditions at the solution of Case I. Increasing UA further, say to* $345kW/K$ *results in an infeasible problem, which we have verified by minimizing the violation of the constraints with a deterministic global optimization routine. Similarly, we can reduce the area down to* $UA=307kW/K$ *and obtain a solution with* $y_1=121.0°C$, $y_2=259.0°C$, *and* $y_3=114.0°C$ *in 31 iterations starting from the conditions at the solution of Case I, but decreasing UA further again results in an infeasible problem. The composite curves for this case are shown in Figure 10(d) for* $UA=340kW/K$ *and Figure 10(e) for* $UA=307kW/K$. *In both scenarios, we see the shape of the lower part of the hot composite curve shift in response to the change in UA, with the pinch point remaining at the same location as in Case I.*

We conclude the description of our new model formulation for MHEXs by underscoring how it can be used as part of a rigorous process design strategy in a way that other existing models cannot. Current simulation-based models are overconstrained in the sense that they allow for only one unknown that can be adjusted to meet two requirements: the energy balance and the second law requirement that heat flows from hot streams to cold streams. In many such models, the adjustable temperature is set by the energy balance, so there is nothing left to adjust to satisfy the second law requirement; it is either satisfied or not based on the values given for the degrees of freedom in the problem, leading to temperature crossovers and other nonphysical solutions. The initial model proposed in the previous section consisting of Eqs. 4 and 15 addresses this issue by enabling the user to specify $\Delta T_{\min}$, thus freeing up two adjustable temperatures to meet the two requirements. It is much easier to specify degrees of freedom that have a feasible solution with this formulation. As noted in Jensen and Skogestad,[24] specifying $\Delta T_{\min}$ is somewhat artificial and can even

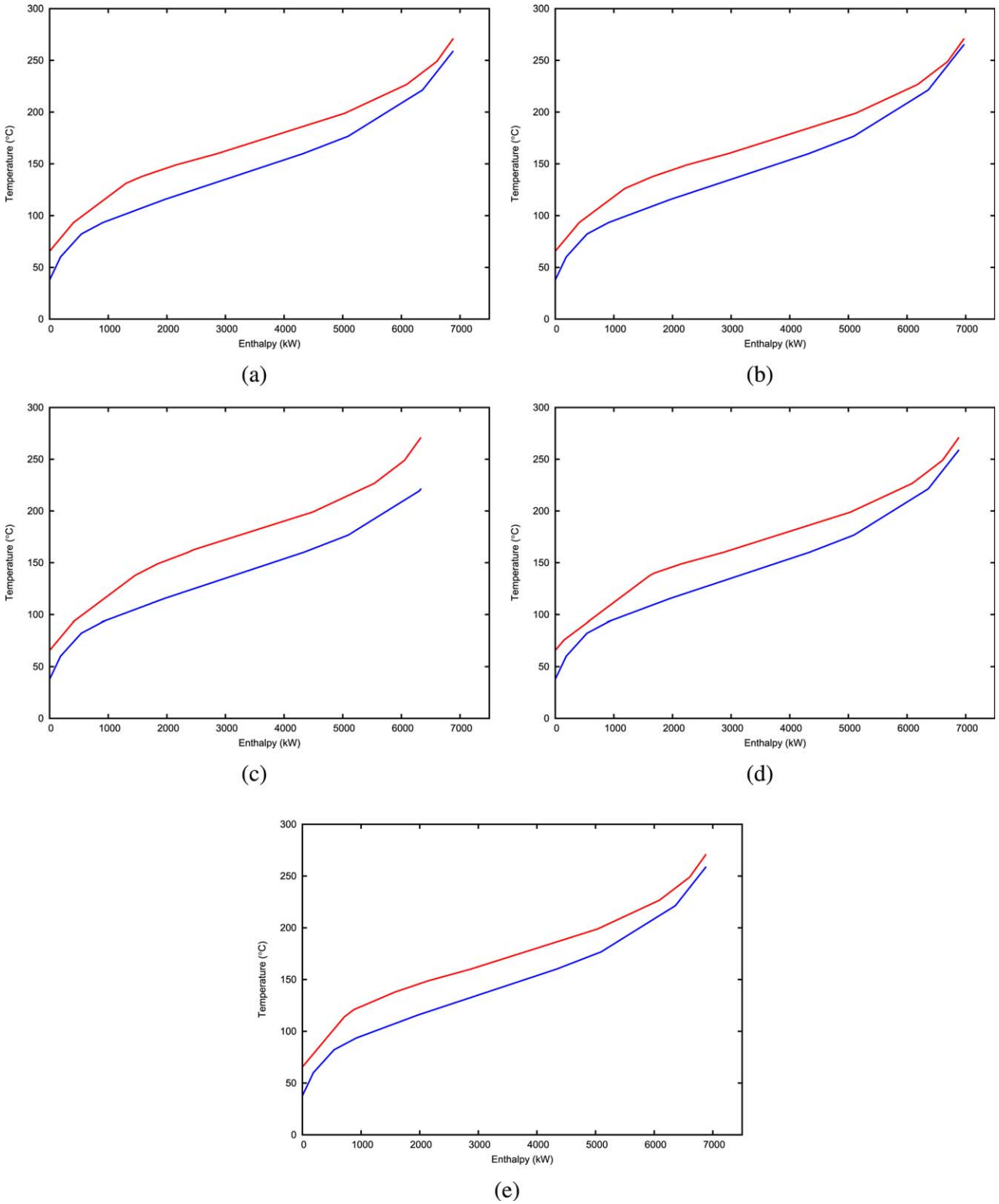

Figure 10. Composite curves of multistream heat exchangers simulated under conditions of (a) Case I, (b) Case II, (c) Case III, (d) Case IV with UA=340 kW/K, (e) Case IV with UA=307 kW/K in Example 4.

[Color figure can be viewed in the online issue, which is available at wileyonlinelibrary.com.]

be counterproductive; it is better thought of as an output of the model, not an input. The three equation model presented here consisting of Eqs. 4, 15 or 23, and 17 addresses this issue by enabling two temperatures and $\Delta T_{\min}$ to be adjustable. However, to make this work, an area (or the product UA) must be specified as a degree of freedom. Again, it is much easier to specify degrees of freedom that have a feasible solution for this formulation, which enables to user to adjust the area to get desirable temperature profiles in the MHEX. However, at the early stages of system design it may not be clear what is a reasonable area to specify. Therefore, the two equation model is very useful at this preliminary stage because the user can

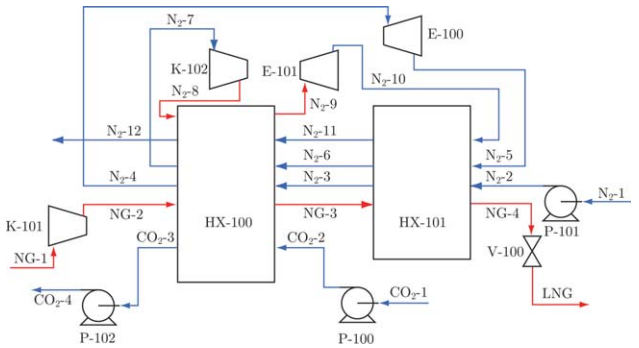

Figure 11. Flowsheet for the LNG process in Example 5 (from Wechsung et al.[25]).

[Color figure can be viewed in the online issue, which is available at wileyonlinelibrary.com.]

specify a reasonable $\Delta T_{\min}$, obtain valid composite curves, and then calculate the corresponding MHEX area (or equivalently use the three equation model with the area as one of the unknowns, as in Case I of Example 4). Once this area is known, the user can use the three equation model with other quantities as unknowns while adjusting the area value around this base value.

LNG Process Case Study

We now present an application of the proposed method to the simulation of a complex LNG production process featuring compression and expansion of process streams as described in Wechsung et al.[25]

Example 5. *A flowsheet for an offshore LNG process is shown in* Figure 11. *Prior to considering heat integration, many of the physical process streams must be split into multiple independent substreams, each with constant heat capacity, to better model the true cooling curves. As in Wechsung et al.,*[25] *the natural gas process stream (NG-x) is split into three separate hot streams (H1-H3), the cold carbon dioxide stream (CO_2-x) is split into two separate cold streams (C1-C2), and the cold nitrogen stream (N_2-x) is split into three cold streams (C3-C5). The remaining process streams are not divided into substreams, resulting in a total of 4 hot streams and 7 cold streams that are considered from the perspective of heat integration in the model. HX-100 handles 3 hot streams and 6 cold streams while HX-101 handles 1 hot stream and 3 cold streams, as detailed in the first three columns of Table* 5.

Table 6. Results for the Different Cases of the LNG Process Case Study

Variable	Case I	Case II	Case III
y_1	365.07 K	365.07 K	365.07 K
y_2	225.44 K	217.66 K	231.10 K
y_3	193.35 K	196.09 K	195.06 K
y_4	95.08 K	95.08 K	95.08 K
y_5	180.85 K	174.75 K	194.58 K
y_6	357.14 K	362.46 K	352.12 K
y_7	95.14 K	91.85 K	97.52 K
y_8	97.54 kW/K	2.62 K	199.06 K
y_9	31.09 kW/K	1.26 K	168.25 K

This problem was originally designed as an optimization problem, so there are too many unknown variables in the formulation from Wechsung et al.[25] to simulate the process. Therefore, some of the variables (namely all of the pressures and flowrates, along with some of the temperatures) are fixed to their values from the solution given in Wechsung et al.[25] which involved no external utilities. Table 5 gives the values of the parameters used in the model as well as the quantities left as unknown variables for this study. There are a total of nine unknowns in the simulation problem: seven temperatures, of which two are solved for by each heat exchanger model and three are solved for by the equations describing the three compression/expansion operations, and two additional variables (one for each MHEX) that we are free to pick as UA, $\Delta T_{\min}$, etc., as shown in the previous example. The compression and expansion operations are modeled as polytropic processes for ideal gases with polytropic exponent $\kappa = 1.352$, as in Wechsung et al.[25]

We now explore several test cases, as in Example 4. As before, we use the CPLEX v12.5 callable library to solve the LP at each iteration and consider the problem to have converged to a solution when the infinity norm of the residual functions is less than 10^{-9}.

Case I. *As a base case, we simulate the process with the variables y_1 through y_7 assigned as in Table* 5, *$y_8 \equiv UA_{\text{HX-100}}$, and $y_9 \equiv UA_{\text{HX-101}}$. $\Delta T_{\min}$ is specified as 4 K for both exchangers. The model converges to the solution shown in the Case I column of Table* 6 *after 128 iterations from the initial guess $\mathbf{y}^0 = [300\ 200\ 100\ 150\ 150\ 100\ 300\ 100\ 100]$. This solution differs slightly from the solution reported in Wechsung et al.,*[25] *however, we note that the authors used the disjunctive formulation from Grossmann et al.,*[9] *whereas we have solved the nonsmooth equations directly, and so a small difference is not unexpected. The*

Table 5. Given Data and Unknown Variables for the Offshore LNG Process Case Study

Stream	Inlet	Outlet	F or $f\left(\frac{\text{kW}}{\text{K}}\right)$	T^{in} or t^{in}(K)	T^{out} or t^{out}(K)	Press.(MPa)
H1	NG-2	NG-3	3.46	319.80	265.15	10.0
H2	NG-2	NG-3	5.14	265.15	197.35	10.0
H3	NG-3	NG-4	3.51	197.35	104.75	10.0
H4	N_2-8	N_2-9	1.03	y_1	y_2	2.7
C1	CO_2-2	CO_2-3	5.19	221.12	252.55	6.0
C2	CO_2-2	CO_2-3	6.10	252.55	293.15	6.0
C3	N_2-2	N_2-3	2.23	103.45	171.05	10.0
C4	N_2-3	N_2-4	1.62	171.05	218.75	10.0
C5	N_2-3	N_2-4	1.06	218.75	221.11	10.0
C6	N_2-6	N_2-7	0.96	y_3	221.15	0.4
C7	N_2-5	N_2-6	0.96	y_4	y_3	0.4
C8	N_2-11	N_2-12	0.93	y_5	y_6	0.1
C9	N_2-10	N_2-11	0.93	y_7	y_5	0.1

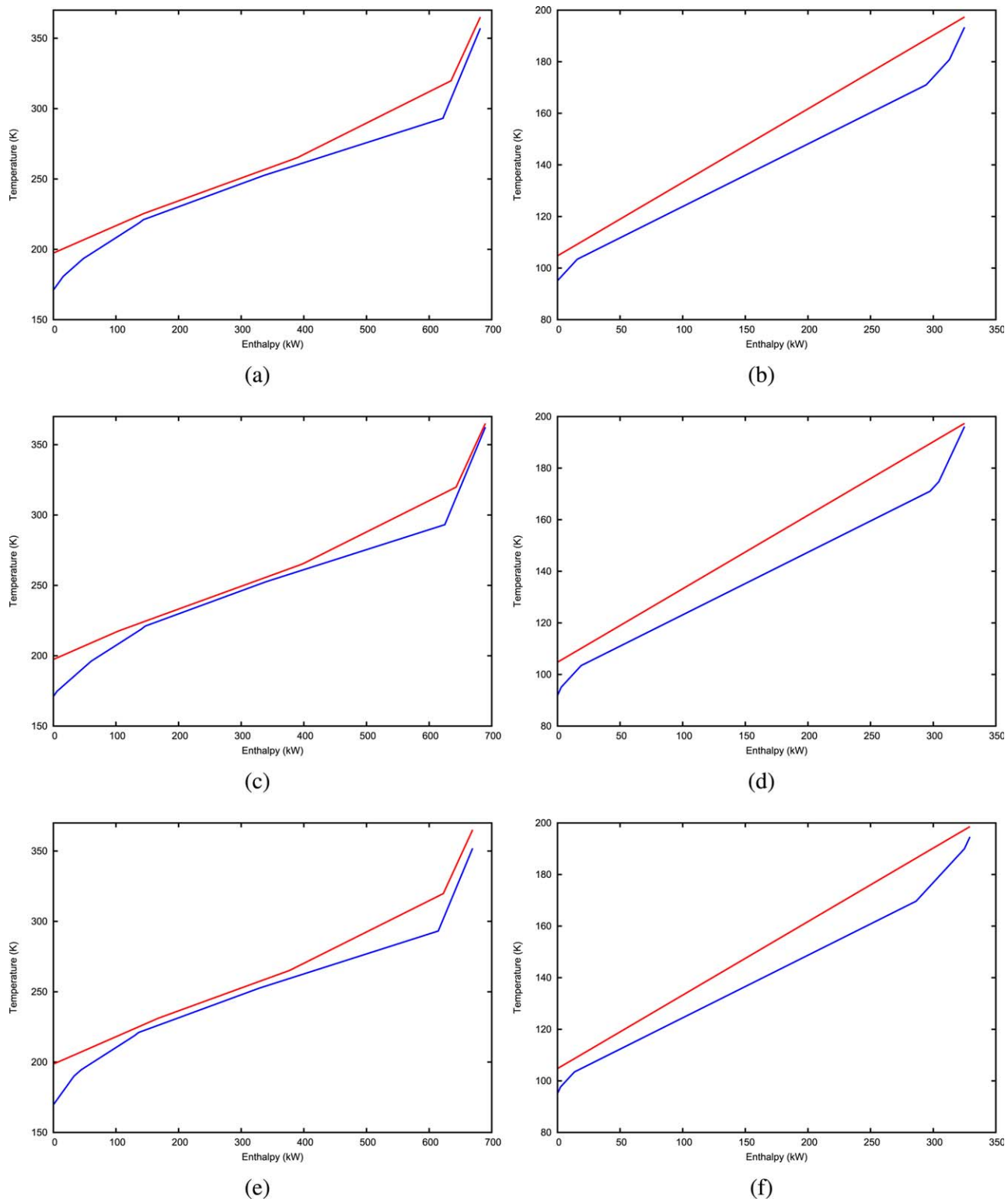

Figure 12. Composite curves of the simulated results of Example 5 under the conditions of (a) Case I for HX-100, (b) Case I for HX-101, (c) Case II for HX-100, (d) Case II for HX-101, (e) Case III for HX-100, (f) Case III for HX-101.

[Color figure can be viewed in the online issue, which is available at wileyonlinelibrary.com.]

composite curves for the two MHEXs in this case are shown in Figure 12a and b.

Case II. *Now we consider a case where the available U $A_{\text{HX-100}}$ is fixed at 120 kW/K, and $UA_{\text{HX-101}}$ is fixed at 30 kW/K. Variables y_1 through y_7 are as assigned as in Table* 5, $y_8 \equiv \Delta T_{\text{min,HX-100}}$, *and* $y_9 \equiv \Delta T_{\text{min,HX-101}}$. *The model converges to the solution given in the Case II column of Table* 6 *after 28 iterations starting from the solution found in Case I. The composite curves for the two MHEXs in this case are shown in* Figure 12c and d. *As can be seen, the curves are more closely pinched together throughout HX-100 than in*

Case I as a result of the increased UA value, with the pinch point location shifting to the high temperature extreme. Note that $\Delta T_{\min,\text{HX-101}}$ also decreases relative to Case I in order to satisfy the overall process model (even though $UA_{\text{HX-101}}$ was specified as a lower value), so the other variable cold outlet temperatures decrease significantly to compensate.

Case III. *Now consider the problem where y_1 through y_7 are as assigned as in Table* 5, *$y_8 \equiv T_{H2}^{\text{out}}$, and $y_9 \equiv t_{C3}^{\text{out}}$. We then specify the $UA_{\text{HX-100}}$=85 kW/K and $UA_{\text{HX-101}}$=35 kW/K. $\Delta T_{\min}$ is specified as 4 K for both exchangers. The model converges to the solution given in the Case III column of Table* 6 *after 48 iterations starting from the solution found in Case I, and the composite curves for this case are shown in* Figure 12e and f. *The reduction in $UA_{\text{HX-100}}$ as compared with Cases I and II leads to larger temperature differences throughout the exchanger than in those simulations, while the increase in $UA_{\text{HX-101}}$ leads to closer temperature approaches in this exchanger (though both exchangers maintain the same pinch points from Case I). However, as in Example 4, the feasibility of the problem is highly dependent on the choices of the UA values. This again highlights the fact that for this particular designation of unknowns and degrees of freedom, there is only a small region in which all the constraints can be satisfied.*

Conclusions

A new method for the simulation and design of processes with MHEXs has been presented, based on recent developments in nonsmooth analysis. While traditional models for multistream heat exchange operations can only be solved for a single unknown variable (using the energy balance), this new model allows for up to three unknown quantities to be calculated simultaneously. The model proposed here also allows for the specification of parameters such as the heat exchange area or the minimum approach temperature as inputs to the model, rather than simply calculating these quantities after the energy balance has already been solved. The nonsmooth equations in these formulations can be solved precisely and with a guaranteed local quadratic convergence rate, owing to the automatic calculation and use of B-subdifferential elements in the equation solving methods. The performance and versatility of the solution procedure has been demonstrated in illustrative examples and on a LNG process flowsheet containing multiple MHEXs in addition to several other process units.

The next step in the current line of work will involve including equations for the detection and simulation of phase changes, which are commonly encountered in cryogenic processes within MHEXs. Future applications involve adapting the model introduced here for other purposes, such as for multistream mass and water exchange networks, as well as including this model in a mathematical programming framework for optimization studies.

Acknowledgments

The authors are grateful to Statoil for providing financial support for this research. We are also grateful to Truls Gundersen at the Norwegian University of Science and Technology (NTNU) for helpful discussions and input.

Notation

A = heat transfer area
AP = pinch location function
C = index set of cold streams
EBP = extended curve pinch location function
F_i = heat capacity flow rate of hot stream i
f_j = heat capacity flow rate of cold stream j
$\mathbf{f}'(\mathbf{y};\mathbf{M})$ = lexicographic directional derivative of $\mathbf{f}$ at $\mathbf{y}$ in the directions $\mathbf{M}$
$\mathcal{F}_{\mathbf{h}}$ = family of continuously differentiable selection functions for the piecewise continuously differentiable functions $\mathbf{h}$
H = index set of hot streams
L = index set for unsorted enthalpy values
K = index set of nondifferentiable (kink) points in and endpoints of the composite curves
P = index set of pinch candidates
P^l = enthalpy in unsorted list entry l
Q^k = enthalpy at nondifferentiable/end point k
Q_C = enthalpy provided by cold utility
Q_H = enthalpy provided by hot utility
T_i^{in} = heat exchanger inlet temperature of hot stream i
t_j^{in} = heat exchanger inlet temperature of cold stream j
T_i^{out} = heat exchanger outlet temperature of hot stream i
t_j^{out} = heat exchanger outlet temperature of cold stream j
T^p = temperature of pinch candidate p
T^k = hot stream temperature at nondifferentiable/end point k
t^k = cold stream temperature at nondifferentiable/end point k
ΔT^k = hot and cold stream temperature difference at nondifferentiable/end point k
ΔT_{LM} = log-mean temperature difference
$\Delta T_{\min}$ = minimum approach temperature between hot and cold streams
U = overall heat transfer coefficient
$\mathbf{y}$ = vector of unknowns in the model
Y = polyhedral set of bounds on the variables $\mathbf{y}$
β = user-defined parameter in smoothing approximation
γ = variable in LP objective of the LP-Newton method
$\partial_B\mathbf{f}(\mathbf{y})$ = B-subdifferential of $\mathbf{f}$ at $\mathbf{y}$
ϕ = selection function, element of $\mathcal{F}_{\mathbf{h}}$

Literature Cited

1. Mokhatab S, Mak JY, Valappil JV, Wood DA. *Handbook of Liquefied Natural Gas*. Houston: Gulf Professional Publishing, 2013.
2. Moniz EJ, Jacoby HD, Meggs AJM. *The Future of Natural Gas: An Interdisciplinary MIT Study*, Cambridge, MA: MIT Press, 2011.
3. Aspen Technology Inc. *Aspen Plus v8.4*. Cambridge, MA: Aspen Technology Inc, 2014.
4. Hasan MMF, Karimi IA, Alfadala HE, Grootjans H. Modeling and simulation of main cryogenic heat exchanger in a base-load liquefied natural gas plant. In: Plesu V, Agachi PS, editors. *17th European Symposium on Computer Aided Process Engineering*, Bucharest, Romania. 2007, pp. 1–6.
5. Hasan MMF, Karimi IA, Alfadala HE, Grootjans H. Operational modeling of MHEXs with phase changes. *AIChE J*. 2009;55(1):150–171.
6. Kamath RS, Biegler LT, Grossmann IE. Modeling MHEXs with and without phase changes for simultaneous optimization and heat integration. *AIChE J*. 2012;58(1):190–204.
7. Duran MA, Grossmann IE. Simultaneous optimization and heat integration of chemical processes. *AIChE J*. 1986;32(1):123–138.
8. Balakrishna S, Biegler L. Targeting strategies for the synthesis and energy integration of nonisothermal reactor networks. *Ind Eng Chem*. 1992;38(3):2152–2164.
9. Grossmann IE, Yeomans H, Kravanja Z. A rigorous disjunctive optimization model for simultaneous flowsheet optimization and heat integration. *Comput Chem Eng*. 1998;22:S157–S164.
10. Lukšan L, Vlček J. Algorithm 811: NDA: Algorithms for Nondifferentiable Optimization. *ACM Trans Math Software*. 2001;27:193–213.
11. Mäkelä MM. Multiobjective Proximal Bundle Method for Nonconvex Nonsmooth Optimization: Fortran Subroutine MPBNGC 2.0. *Reports of the Department of Mathematical Information Technology, Series B, Scientific Computing*. University of Jyväskylä, Jyväskylä, 2003;(B 13/2003).
12. Facchinei F, Pang JS. *Finite-Dimensional Variational Inequalities and Complementarity Problems*, Vol.2. New York, NY: Springer-Verlag New York, Inc. 2003.
13. Facchinei F, Fischer A, Herrich M. An LP-Newton method: nonsmooth equations, KKT systems, and nonisolated solutions. *Math Program*. 2014;146:1–36.

14. Khan KA, Barton PI. A vector forward mode of automatic differentiation for generalized derivative evaluation. *Optimization Methods and Software*, DOI: 10.1080/10556788.2015.1025400.
15. Griewank A, Walther A. *Evaluating Derivatives: Principles and Techniques for Algorithmic Differentiation*, 2nd ed. Philadelphia, PA: SIAM, 2008.
16. Griewank A. Automatic directional differentiation of nonsmooth composite functions. In: Durier R, Michelot C, editor. *Recent Developments in Optimization, vol. 429 of Lecture Notes in Economics and Mathematical Systems*, Berlin Heidelberg: Springer, 1995, pp. 155–169.
17. Khan KA, Barton PI. Evaluating an element of the Clarke generalized Jacobian of a composite piecewise differentiable function. *ACM Trans Math Software*. 2013;39(4):1–28.
18. Smith R. *Chemical Process Design*. New York: McGraw-Hill, Inc, 1995.
19. Hewitt GF, Pugh SJ. Approximate design and costing methods for heat exchangers. *Heat Transfer Eng*. 2007;28(2):76–86.
20. Khan KA. Sensitivity Analysis for Nonsmooth Dynamic Systems. Ph.D. thesis, Massachusetts Institute of Technology, Cambridge, MA, 2014.
21. Zavala-Río A, Femat R, Santiesteban-Cos R. An analytical study of the logarithmic mean temperature. *Revista Mexicana de Ingeniería Químca*. 2005;4:201–212.
22. Chakraborty S, Ghosh P. Heat exchanger network synthesis: the possibility of randomization. *Chem Eng J*. 1999;72:209–216.
23. IBM. IBM ILOG CPLEX v12.5. Available at: http://www-01.ibm.com/software/commerce/optimization/cplex-optimizer/index.html), 2015. Accessed on March 10, 2015.
24. Jensen JB, Skogestad S. Problems with specifying ΔT_{min} in the design of processes with heat exchangers. *Ind Eng Chem Res*. 2008; 47:3071–3075.
25. Wechsung A, Aspelund A, Gundersen T, Barton PI. Synthesis of heat exchanger networks at subambient conditions with compression and expansion of process streams. *AIChE J*. 2011;57(8):2090–2108.

Manuscript received May 1, 2015, and revision received July 6, 2015.